
Project Report

POLYTECHNIQUE
MONTRÉAL

UNIVERSITÉ
D'INGÉNIERIE



Attitude determination of a satellite
using a gyroscope and two star trackers

ELE6209A - Systèmes de Navigation

Winter 2022

Département de génie électrique
École Polytechnique de Montréal

Dernière mise à jour: April 29, 2022

Adam **Ghribi**

2161271

Jacques **Desfossés**

61902

1 Introduction

Satellites used for optical and radar measurements have strict requirements on attitude accuracy. A main part of the attitude and orbit control subsystem (AOCS) is dedicated to the estimation of the spacecraft's orientation using an accurate and reliable navigation system. In this project, we determine the attitude of a satellite in a circular equatorial low earth orbit (300 km) using a navigation system equipped with two types of sensors. The first sensor is a high-rate gyroscope which provides angular velocity measurements and thus operates as a dead reckoning sensor. The other two sensors are lower-rate star trackers whose role is to supply aiding attitude measurements used for position fixing. This combination of sensors has been selected due to its common use in real-life satellite navigation systems.

In the work that follows, we first describe the satellite's navigation system. We then explain the design of the Multiplicative Extended Kalman Filter (MEKF) which has been selected as the fusion algorithm. Finally, the simulated results are presented along with an analysis of the system's performance.

2 System Description

The satellite's navigation system relies on a gyroscope and two star trackers. This particular combination of sensors is commonly used for the attitude estimation of space crafts although spatial navigation systems often include additional and redundant sensors for greater reliability. This navigation system is a modified version of the system examined by [MC14, Chapter 6]. The differences lie in the gyroscope's bias dynamics modeled as a first-order Markov process, as done by [Le 22], and in the way the star tracker measurements are fused. The performance expected from the navigation system is an attitude estimation with a precision of one arc second or less given the high accuracy specifications of the selected sensors.

In this section, we describe the various frames of reference used to determine the attitude of the satellite as well as their relation with each other (rotation matrix) when needed. We also present the mathematical model of the different sensors.

2.1 Frames of Reference

2.1.1 Earth Centered Inertial (ECI) Frame

The gyro sensor used in the navigation system is an inertial sensor which means that it provides measurements with respect to an inertial frame, i.e. a non-accelerating frame of reference in which the Newton's laws of motion apply. The Earth Centered Inertial (ECI) frame is the inertial frame relative to which the gyro will produce measurements and is denoted $\{i\}$. Conveniently, the star trackers also report the attitude of the spacecraft with respect to the ECI frame. The origin of the ECI frame is located at the center of mass of the Earth. The x_i axis points towards the vernal equinox whereas the z_i axis points towards the North Pole and is therefore along the Earth's spin axis. The y_i axis is defined to complete the right-handed coordinate system.

2.1.2 Orbit/Navigation Frame

The orbit frame moves with the satellite and corresponds to the navigation frame. This frame is denoted $\{n\}$. Its origin is located at the satellite's center of mass. The x_n axis points towards the direction of motion. The z_n axis is the nadir and points towards the center of mass of the Earth. The y_n axis is defined to complete the right-handed coordinate system and is normal to the orbital plane. By definition, the satellite's velocity vector $v^n(t)$ and the axis z_n are always perpendicular because the orbit of interest is circular. This frame of reference also corresponds to the local vertical/local horizontal (LVLH) frame commonly used in orbital mechanics.

2.1.3 Body Frame

The body frame is fixed to the satellite and is denoted $\{b\}$. Its origin is located at the satellite's center of mass. The z_b axis goes from the top to the bottom of the satellite and points towards the center of mass of the Earth (down). The x_b axis points from the back to the front of the satellite (forward). The y_b axis is defined to complete the right-handed coordinate system. The body frame is aligned with the navigation frame when the satellite has an attitude of 0° in roll, pitch and yaw. The deviation between the body frame and the navigation frame describes the satellite's attitude.

2.2 Rotation From ECI to the Navigation Frame

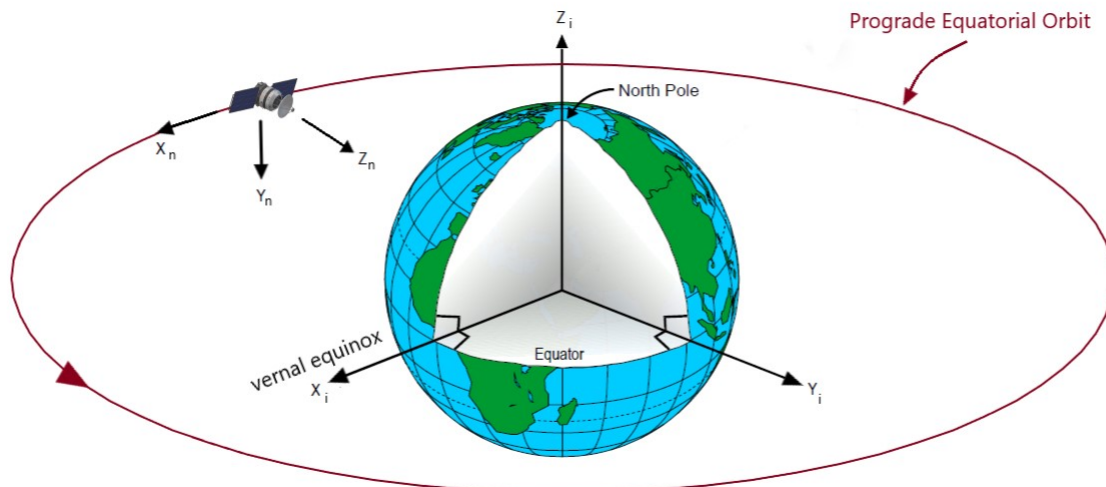


Figure 1: ECI and navigation frames of reference for the selected orbit. Modified from [©2011 FAA, CC BY-SA 3.0, via Wikimedia Commons]

The rotation matrix $R_i^n(t)$ will be needed to convert, to the navigation frame, the attitude estimates of the body frame $\{b\}$ computed with respect to the ECI frame $\{i\}$. This rotation matrix depends

on the position vector $\frac{\mathbf{r}^n(t)}{\|\mathbf{r}^n(t)\|} = -\mathbf{z}_n$ and velocity vector $\frac{\mathbf{v}^n(t)}{\|\mathbf{v}^n(t)\|} = \mathbf{x}_n$ of the satellite. In order to simplify this transformation, a circular equatorial prograde orbit, shown in Figure 1, has been selected. For such orbits, the orbital plane coincides with the geocentric equatorial plane and $\mathbf{y}_n = -\mathbf{z}_i$. The period T of the circular orbit of radius R is [Cur21]

$$T = 2\pi \sqrt{\frac{R^3}{\mu}} \quad (1)$$

Where $\mu = 3.986 \times 10^5 \text{ km}^3/\text{s}^2$ is the gravitational parameter of the Earth. For our simulations, we set the position of the satellite at time t_0 to be on the vernal equinox axis when $\mathbf{x}_i = \mathbf{z}_n$. As a result, the angle $\theta(t)$ between the vernal equinox axis \mathbf{x}_i and the \mathbf{z}_n axis of the navigation frame can be written as

$$\theta(t) = \frac{2\pi}{T}t = \sqrt{\frac{\mu}{R^3}}t \quad (2)$$

The rotation matrix $R_n^i(t)$ can be expressed as

$$R_n^i(t) = \begin{bmatrix} \sin(\theta(t)) & 0 & \cos(\theta(t)) \\ -\cos(\theta(t)) & 0 & \sin(\theta(t)) \\ 0 & -1 & 0 \end{bmatrix} \quad (3)$$

And the desired matrix $R_i^n(t) = (R_n^i(t))^T$ is

$$R_i^n(t) = \begin{bmatrix} \sin(\theta(t)) & -\cos(\theta(t)) & 0 \\ 0 & 0 & -1 \\ \cos(\theta(t)) & \sin(\theta(t)) & 0 \end{bmatrix} \quad (4)$$

We can also give an expression for $\omega_{n/i}^n$, the angular velocity vector of the navigation frame $\{n\}$ with respect to the ECI frame, represented in the navigation frame. We have

$$\omega_{n/i}^n = \begin{bmatrix} 0 & -\sqrt{\frac{\mu}{R^3}} & 0 \end{bmatrix}^T \quad (5)$$

For navigation systems where the navigation frame is a NED frame which rotates with the Earth, $\omega_{n/i}^n$ and R_n^i are not obtained as easily and the former is often treated as noise in the system [Le 22].

2.3 Sensors

2.3.1 Three-Axis Gyroscope

The gyroscope measures $\omega_{b/i}^p$, the angular velocity vector of the satellite frame $\{b\}$ with respect to the Earth Centered Inertial (ECI) frame, represented in the platform frame $\{p\}$. For simplicity, we will assume that the satellite frame is aligned with the platform frame. As a result $R_p^b = I_3$ and we can express the gyro measurements as $\omega_{b/i}^b$.

The three-axis gyro is modeled using the continuous-time mathematical model described by [Le 22] and given as

$$\tilde{\boldsymbol{\omega}}_{\text{b/i}}^{\text{b}} = \boldsymbol{\omega}_{\text{b/i}}^{\text{b}} + H_{\omega} \boldsymbol{x}_{\omega} + \boldsymbol{\nu}_{\omega} \quad (6)$$

$$\dot{\boldsymbol{x}}_{\omega} = F_{\omega} \boldsymbol{x}_{\omega} + \boldsymbol{\nu}_{\boldsymbol{x}_{\omega}} \quad (7)$$

where $\boldsymbol{\nu}_{\omega}$ is a Gaussian white noise with PSD $\sigma_{\boldsymbol{\nu}_{\omega}}^2$, $H_{\omega} \boldsymbol{x}_{\omega}$ is an additive error and \boldsymbol{x}_{ω} is the gyro state to be estimated. The dynamics of the gyro state are modeled by 7 where $\boldsymbol{\nu}_{\boldsymbol{x}_{\omega}}$ is a Gaussian white noise with PSD $\sigma_{\boldsymbol{x}_{\omega}}^2$. In order to obtain an additive bias for the gyro, we are setting $F_{\omega} = -\lambda_{\omega} I_3$ and $H_{\omega} = I_3$. The gyroscope data used for simulation is summarized in Table 1. Note that the gyroscope's bias dynamics model allows the specification of the time constant λ_{ω} . This is an enhancement over the MEKF used as reference [MC14] which requires $\lambda_{\omega} = 0$ and models the gyroscope's bias dynamics as a Weiner process [Dev98].

Table 1: Gyroscope data used for simulation

Description	Variable	Value	Units
Measurement rate	f_{ω}	10	Hz
Initial bias	$\text{Var}(\boldsymbol{x}_{\omega}(0))$	$(0.1)^2$	$(^{\circ}/hr)^2$
Initial bias covariance	$\Sigma(\boldsymbol{x}_{\omega}(0))$	$(0.2)^2$	$(^{\circ}/hr)^2$
Gyro noise PSD	$\sigma_{\boldsymbol{x}_{\omega}}^2$	$\sqrt{10} \cdot 10^{-6}$	$(rad/s)/\sqrt{Hz}$
Bias noise PSD	$\sigma_{\boldsymbol{\nu}_{\omega}}^2$	$\sqrt{10} \cdot 10^{-10}$	$(rad/s^2)/\sqrt{Hz}$
Bias time constant	λ_{ω}	1/60	1/s

2.3.2 Star Trackers



Figure 2: Sodern's Hydra star tracker. [©2013 Christian Lafont, CC BY-SA 3.0, via Wikimedia Commons]

Two star trackers provide attitude aiding measurements. A star tracker (STR) is a high accuracy sensor which captures images of stars and compares their pattern with the known pattern of stars in the sky to determine the satellite's attitude in the ECI frame, i.e. R_b^i since the platform frame is aligned with the body frame. The sensor's accuracy depends on several factors such as the number of stars that it can track, its star map and the quality of its optical components. The star tracker shown on Figure 2 was developed by the French company Sodern and has a precision of one arc second on each of its three axes [Wik22].

A star tracker has two modes of operation: tracking mode and initial attitude acquisition [MC14]. The initial acquisition mode is sometimes identified as "lost-in-space" mode on the instrument's data sheet. During acquisition, the star tracker searches the entire field of view to identify star patterns and the attitude determination takes a few seconds to complete. In tracking mode, the sensor tracks stars that have already been identified and matched with stars in its catalog. The attitude determination in tracking mode is therefore faster than the initial attitude acquisition. The angle measurements provided by the sensor are described by [Win][XGM22] and given as

$$\tilde{\Phi}_b^i = \begin{bmatrix} \tilde{\phi} \\ \tilde{\theta} \\ \tilde{\psi} \end{bmatrix} = \Phi_b^i + \boldsymbol{\nu}_{\Phi} = \begin{bmatrix} \phi \\ \theta \\ \psi \end{bmatrix} + \begin{bmatrix} \nu_{xy} \\ \nu_{xy} \\ \nu_z \end{bmatrix} \quad (8)$$

where ϕ , θ and ψ are respectively the roll, pitch and yaw angles while ν_{xy} and ν_z are zero-mean Gaussian white noises with variance σ_{xy}^2 and σ_z^2 . Star trackers typically provide better accuracy in

the cross-boresight pointing directions [MC14]. In such cases, the star tracker noise is modeled with $\sigma_z^2 > \sigma_{xy}^2$. However, for simplicity, the noise in our simulations will be the same in all directions and equal to σ_{STR}^2 .

Table 2: Star tracker data used for simulation

Description	Variable	Value	Units
Measurement rate	f_{STR}	0.5	Hz
Attitude noise variance	$\sigma_{STR}^2 = \sigma_{xy}^2 = \sigma_z^2$	0.2 ²	arcsec ²
Initial attitude covariance	$\Sigma(\delta\phi(0))$	6 ²	arcsec ²

Fusion of Star Trackers

We opted to fusion two star trackers to improve the accuracy of the aiding measurements. To that extent, we used the method proposed by [Win] which will be repeated next for convenience. We consider two scalar measurements z_1 and z_2 from different two sensors where

$$z_1 = x + \eta_1 \quad (9)$$

$$z_2 = x + \eta_2 \quad (10)$$

We consider then $\mathbf{z} = [z_1 \ z_2]^T$ and $\boldsymbol{\eta} = [\eta_1 \ \eta_2]^T$. The goal is to estimate x where

$$\mathbf{z} = H\mathbf{x} + \boldsymbol{\eta} \quad (11)$$

$$\text{with } E[\boldsymbol{\eta}\boldsymbol{\eta}^T] = R = \begin{bmatrix} \sigma_1^2 & 0 \\ 0 & \sigma_2^2 \end{bmatrix}, \text{ and } E[\boldsymbol{\eta}] = [0 \ 0]^T \quad (12)$$

The minimum variance estimate \hat{x} is given by

$$\hat{x} = (H^T R^{-1} H)^{-1} R^{-1} \mathbf{z} \quad (13)$$

The estimation error covariance matrix is given as

$$P = (H^T R^{-1} H)^{-1} = \frac{1}{\frac{1}{\sigma_1^2} + \frac{1}{\sigma_2^2}} = \frac{\sigma_1^2 \sigma_2^2}{\sigma_1^2 + \sigma_2^2} \quad (14)$$

Which proves that $P < \sigma_1^2$ and $P < \sigma_2^2$. By assuming that both star sensors are identical, and that their noise components ν are not correlated we obtain $P = \frac{\sigma_{STR}^2}{2}$, where $\sigma_{STR} = \sigma_1 = \sigma_2$.

To validate the results, we performed 1000 simulations and we measured the roll angle ϕ using two star trackers. The results are shown on Figure 3. We can clearly see that by using two sensors we are able to reduce the drift. The variance obtained with two star trackers is indeed half of the variance obtained with a single star tracker.

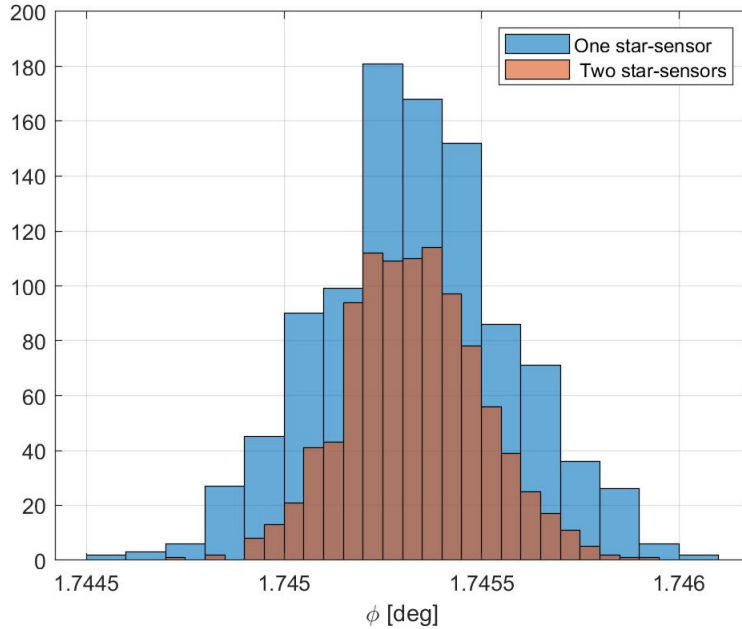


Figure 3: Deviation of the star tracker measurements

3 Attitude Estimation

In this section, we describe our proposed solution to fuse the data of the gyro and the two star trackers in order to estimate the satellite's orientation. Our approach is based on the Multiplicative Extended Kalman Filter (MEKF) described in [MC14]. The goal is to estimate the attitude quaternion q_b^i . We define the error in a multiplicative form as $\delta q = q_b^i * (\hat{q}_b^i)^{-1}$, and we determine a minimal three-independent-component state vector representation $\delta\phi$ of this error, which we estimate using the MEKF.

3.1 The Mechanization Equations

We use the mathematical notations mentioned by [Le 22]. To simplify the notation, let us set $q = q_b^i$, $\omega^i = \omega_{b/i}^i$, and $\omega = \omega_{b/i}^b$. We start by differentiating the multiplicative error defined above.

We obtain

$$\begin{aligned}
 \delta\dot{q} &= \dot{q} * \hat{q}^{-1} + q * \dot{\hat{q}}^{-1} \\
 &= \frac{1}{2}\boldsymbol{\omega}^i * q * \hat{q}^{-1} - q * \hat{q}^{-1} * \dot{\hat{q}} * \hat{q}^{-1} \\
 &= \frac{1}{2}\boldsymbol{\omega}^i * \delta q - \frac{1}{2}\delta q * \hat{\boldsymbol{\omega}}^i \\
 &= \frac{1}{2}\delta q * \boldsymbol{\omega} - \frac{1}{2}\hat{\boldsymbol{\omega}} * \delta q
 \end{aligned} \tag{15}$$

We then write the differential equation as follows

$$\delta\dot{q} = \frac{1}{2} \begin{bmatrix} 0 & (\hat{\boldsymbol{\omega}} - \boldsymbol{\omega})^T \\ \boldsymbol{\omega} - \hat{\boldsymbol{\omega}} & -[\hat{\boldsymbol{\omega}} + \boldsymbol{\omega}]_{\times} \end{bmatrix} \delta q \tag{16}$$

For small attitude variations [Le 22], we can use the approximation $\delta q^T \approx [1 \ \frac{1}{2}\boldsymbol{\delta\phi}^T]$. From 16 we obtain

$$\begin{bmatrix} 1 \\ \frac{1}{2}\boldsymbol{\delta\dot{\phi}} \end{bmatrix} = \begin{bmatrix} 0 & (\hat{\boldsymbol{\omega}} - \boldsymbol{\omega})^T \\ \boldsymbol{\omega} - \hat{\boldsymbol{\omega}} & -[\hat{\boldsymbol{\omega}} + \boldsymbol{\omega}]_{\times} \end{bmatrix} \begin{bmatrix} 1 \\ \frac{1}{2}\boldsymbol{\delta\phi} \end{bmatrix} \tag{17}$$

Substituting $\boldsymbol{\omega} = \hat{\boldsymbol{\omega}} + \boldsymbol{\delta\omega}$ into 17, where $\boldsymbol{\delta\omega}$ is the angular rate error, we get

$$\boldsymbol{\delta\dot{\phi}} = \boldsymbol{\delta\omega} - \frac{1}{2}[\hat{\boldsymbol{\omega}} + \boldsymbol{\omega}]_{\times}\boldsymbol{\delta\phi} \tag{18}$$

We now define the gyro state error as $\boldsymbol{\delta x}_{\omega} = \boldsymbol{x}_{\omega} - \hat{\boldsymbol{x}}_{\omega}$. We obtain the following navigation equations

$$\begin{cases} \boldsymbol{\delta\dot{\phi}} = -H_{\omega}\boldsymbol{\delta x}_{\omega} - \boldsymbol{\nu}_{\omega} - [\hat{\boldsymbol{\omega}} + \frac{1}{2}\boldsymbol{\delta\omega}]_{\times}\boldsymbol{\delta\phi} \\ \boldsymbol{\delta\dot{x}}_{\omega} = F_{\omega}\boldsymbol{\delta x}_{\omega} + \boldsymbol{\nu}_{x_{\omega}} \end{cases} \tag{19}$$

The state vector is composed by the minimized quaternion error $\boldsymbol{\delta\phi}$ and the gyro state error $\boldsymbol{\delta x}_{\omega}$ and is

$$\boldsymbol{\delta x}(t) = \begin{bmatrix} \boldsymbol{\delta\phi}(t) \\ \boldsymbol{\delta x}_{\omega}(t) \end{bmatrix} \in \Re^6 \tag{20}$$

Denoting estimates with a hat symbol, the mechanization equations are finally

$$\begin{cases} \boldsymbol{\delta\dot{\hat{\phi}}} = [-\hat{\boldsymbol{\omega}}]_{\times}\boldsymbol{\delta\hat{\phi}} \\ \boldsymbol{\delta\dot{\hat{x}}}_{\omega} = 0 \end{cases} \tag{21}$$

3.2 Linearized Error Model

3.2.1 Error Dynamics

The linearization of 21 leads to the following differential equation

$$\boldsymbol{\delta\dot{x}} = A(t)\boldsymbol{\delta x}(t) + B\boldsymbol{\nu} \tag{22}$$

where $\boldsymbol{\nu}^T = [\boldsymbol{\nu}_{\omega}^T \ \boldsymbol{\nu}_{x_{\omega}}^T]$ and:

$$A(t) = \left[\begin{array}{c|c} [-\hat{\boldsymbol{\omega}}]_{\times} & -H_{\omega} \\ \hline 0_{3 \times 3} & F_{\omega} \end{array} \right], \quad B = \left[\begin{array}{c|c} -I_{3 \times 3} & 0_{3 \times 3} \\ \hline 0_{3 \times 3} & I_{3 \times 3} \end{array} \right] \tag{23}$$

3.2.2 Aiding Measurements

The measures from the star trackers are Euler angles. To update our estimate, we transform the Euler angles to an attitude quaternion and compute the angle error $\delta\tilde{\phi}$ from the estimated orientation. We use the following formula derived by [MC14]

$$\mathbf{y}_k = \boldsymbol{\delta}\phi_k = 2 \frac{[q * (\hat{q}_k^-)^{-1}]_{1:3}}{[q * (\hat{q}_k^-)^{-1}]_0} \quad (24)$$

The equation is linear in $\boldsymbol{\delta}\mathbf{x}$. We obtain

$$C = [I_{3 \times 3} \quad 0_{1 \times 3}] \quad , \quad D = I_{3 \times 3} \quad (25)$$

The measurement covariance matrix R is a 3×3 matrix of the attitude measurement error angles. By using 8 we assume that $R = E[\boldsymbol{\nu}_\Phi \boldsymbol{\nu}_\Phi^T]$.

3.3 Summary of the Filter Design

Our MEKF is based on the design described by [MC14] and the techniques covered by [Le 22]. First, we initialize the attitude quaternion q , the covariance matrix Σ , the angular rate ω , and the bias \mathbf{x}_ω . Then, we integrate the state and propagate the covariance matrix. In a second step, we compute the Kalman gain and update the measurements. Finally, we estimate the orientation and reset the error to zero. Our approach is summarized below.

(i) Initialization and Propagation The estimated quaternion kinematics equations are described by [Le 22] and given as

$$\dot{\hat{q}} = \frac{1}{2} \left[-\hat{q}^T \quad \hat{q}_0 I_{3 \times 3} - [\hat{q}]_\times \right] \hat{\omega} \quad (26)$$

We initialize $\hat{q}_k(t_0) = q_0$, $\hat{\mathbf{x}}_\omega(t_0) = \mathbf{x}_{\omega 0}$, and $\Sigma(t_0) = \Sigma_0$. We then compute \hat{q}_k^- by integrating 26. The estimated angular rate is given by $\hat{\omega} = \tilde{\omega} - H_\omega \hat{\mathbf{x}}_\omega$. To propagate the covariance, we solve the following differential equation

$$\dot{\Sigma}(t) = A(t)\Sigma(t) + \Sigma(t)A^T(t) + BQB^T \quad (27)$$

where $Q = E[\boldsymbol{\nu} \boldsymbol{\nu}^T]$. To do so, We define the matrices Φ_i and N_i given as

$$\Phi_i = e^{A_i \delta\tau_i} \quad , \quad N_i \approx \delta\tau_i BQB^T$$

where we divide the interval $[t_{k-1}, t_k]$ between the measurements into integration subintervals $t_{k-1} = \tau_0 < \dots < \tau_i < \dots < \tau_n = t_k$. In each substep we have

$$\Sigma_{i+1} = \Phi_i \Sigma_i \Phi_i^T + N_i ; \quad i = 0 \dots n-1$$

After propagation, we obtain $\Sigma_k^- = \Sigma_n$.

(ii) Gain Calculation We compute the Kalman gain with

$$K_k = \Sigma_k^- C^T [C \Sigma_k^- C^T + R]^{-1} \quad (28)$$

(iii) Measurement Update We update the covariance matrix and the error state vector as follows

$$\Sigma_k^+ = (I_6 - K_k C) \Sigma_k^- \quad (29)$$

$$\delta \hat{x}_k^+ = K_k \left[y_k - 2 \frac{[\hat{q}_k^- * (\hat{q}_k^-)^{-1}]_{1:3}}{[\hat{q}_k^- * (\hat{q}_k^-)^{-1}]_0} \right] = K_k y_k \quad (30)$$

(iv) Reset We update the estimates of the attitude quaternion and the gyro state. According to [MC14] the quaternion update can be accomplished in two steps

$$q^* = \hat{q}_k^- + \frac{1}{2} \begin{bmatrix} -\hat{q}_k^{-T} \\ \hat{q}_{0k}^- I_{3 \times 3} - [\hat{q}_k^-]_\times \end{bmatrix} \delta \hat{\phi}^+ \quad (31)$$

$$\hat{q}_k^+ = \frac{q^*}{\|q^*\|} \quad (32)$$

We compute the gyro state as follows

$$\hat{x}_{\omega k}^+ = \hat{x}_{\omega k}^- + \delta \hat{x}_{\omega k}^+ \quad (33)$$

Finally, we reset $\delta \hat{x}_k$ to zero and repeat all the steps starting from (i) by taking our estimates as initial values.

4 Simulation

4.1 Setup

The simulation data specific to the gyroscope and the two star trackers is given in Tables 1 and 2. The remaining simulation parameters summarized in Table 3. Note that the simulation time of 90 min is approximately the period of a satellite in a circular orbit around the Earth at an altitude of 300 km. The exact period is 90.5 min when computed with equation 1. Also, the fusion of the star trackers is done before filtering, using equation 14. This implies that during the simulation, both star trackers are effectively treated as a single sensor with improved accuracy.

Table 3: Simulation parameters

Description	Variable	Value	Units
Simulation duration	t_{sim}	90	min
True initial quaternion	$q_b^i(0)$	$\sqrt{2}/2 \begin{bmatrix} 1 & 0 & 0 & 1 \end{bmatrix}^T$	
True angular velocity	$\omega_{b/i}^b(t)$	$0.1 \begin{bmatrix} \sin(0.01t) \\ \sin(0.0085t) \\ \cos(0.0085t) \end{bmatrix}$	°/s

The simulations are performed in mission mode, meaning that the system's initial orientation has been obtained from the star trackers' attitude initialization mode and the initial covariance reflects its uncertainty.

4.2 Analysis of the Results

In this section, we present and analyse our results. The fusion of the star trackers and the gyro using the MEKF described in section 3.3 provides an estimate of the satellite's attitude and gyro biases. We compare the filter outputs with the true orientation and gyro state by analysing the estimation errors.

We set the measurement-update frequency of the star trackers to 2 Hz , i.e. (1/5 times the gyro measurement frequency) and the filter frequency to 10 Hz (same as the gyro).

We first examine the system with $\lambda_\omega = 0$. For the attitude estimation, we see in Fig. 4 that the filtered data follows the true Euler angles. The attitude error indeed shows that the system can achieve a pointing accuracy level of 0.3 arcsec . The red curves on the error plots correspond to the $3\sigma_{STR}$ values. These lines have been plotted for reference only and do not provide information on the statistics of the error.

However, Figure 5 shows that the algorithm is unable to estimate the gyro biases. We see that the error does not converge or oscillate around the expected bias. Due to this problem, we are unable to determine the attitude accurately for simulations longer than 2 hours as the system becomes unstable.

To improve our results, we adjust the gyro model by setting $\lambda_\omega = 1/60\text{s}^{-1}$. So that the integrated gyro state should converge exponentially to zero. Fig. 6 demonstrates a lower bias but different from the expected value. The accuracy of the attitude estimation is slightly improved but still unstable for long simulation periods.

In conclusion, we can assume that the navigation system generates acceptable Euler angles estimates during one orbit. We recommend however to improve and adjust the gyro model. The results show that a good bias estimate is crucial for a performant MEKF. In our case, we need to calibrate the system after each orbit to ensure acceptable filter outputs. For long period mission modes longer than 90min , it is difficult to achieve acceptable high performance without adjusting the gyro parameters.

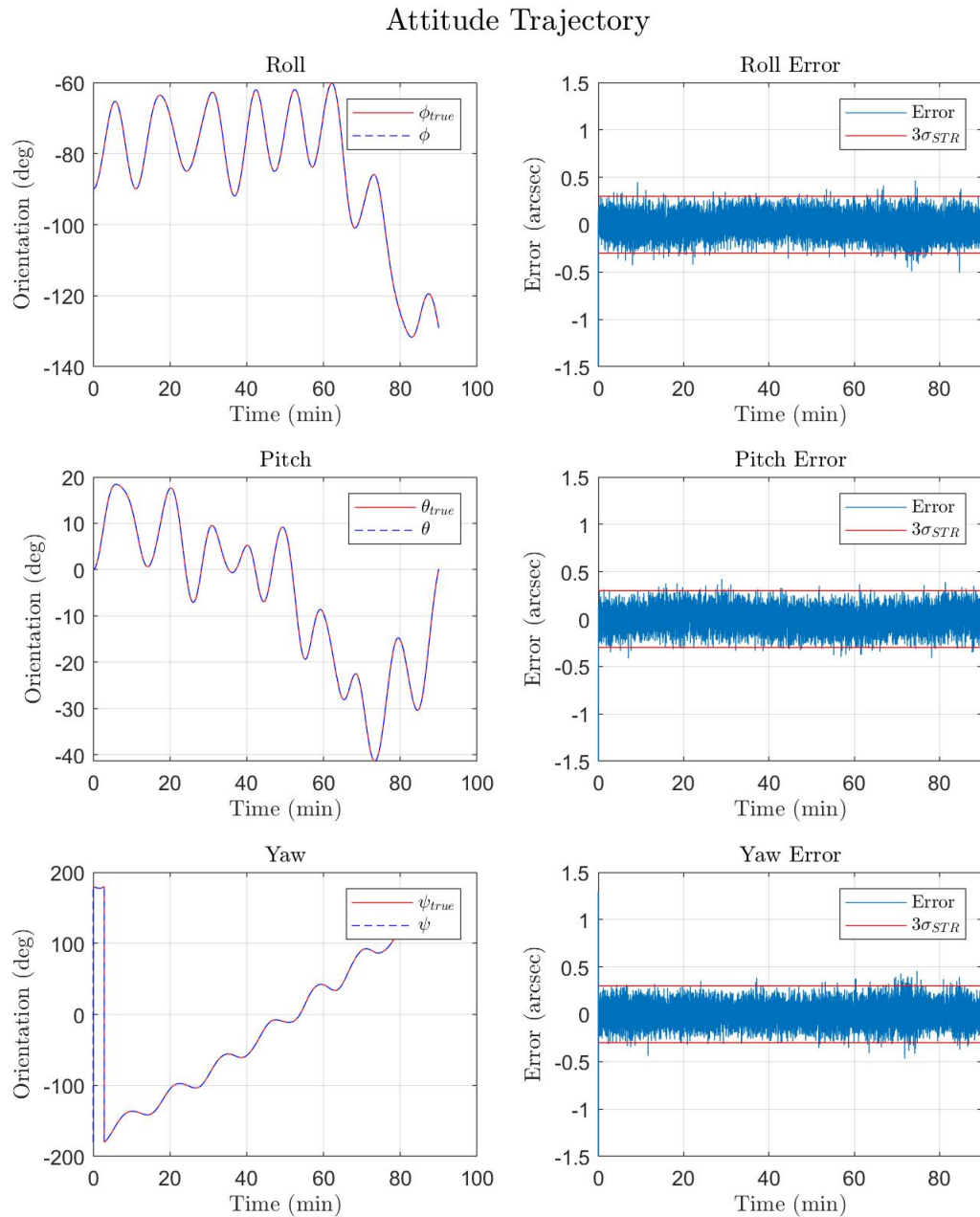


Figure 4: Deviation of the star tracker measurements

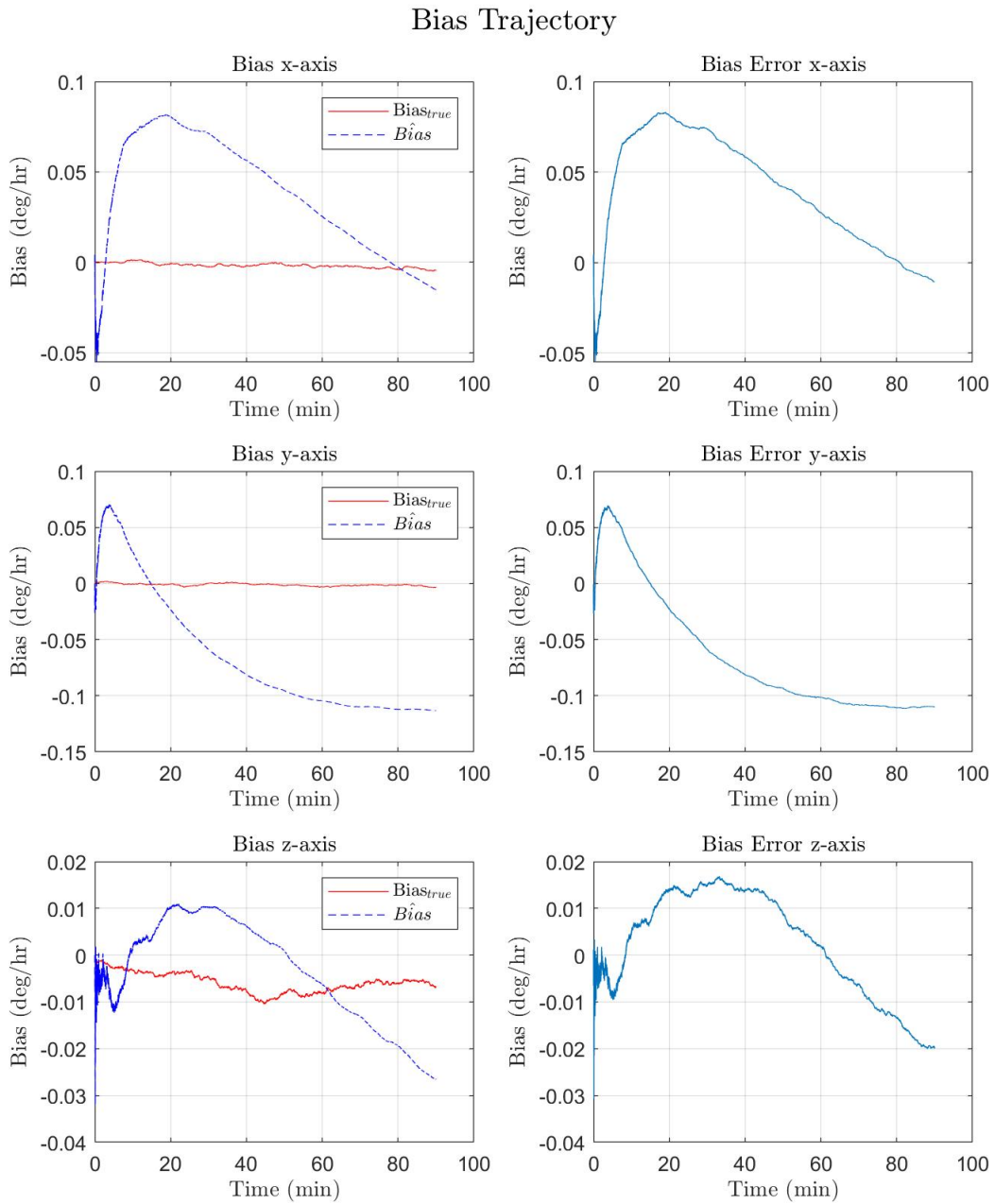


Figure 5: Deviation of the star tracker measurements

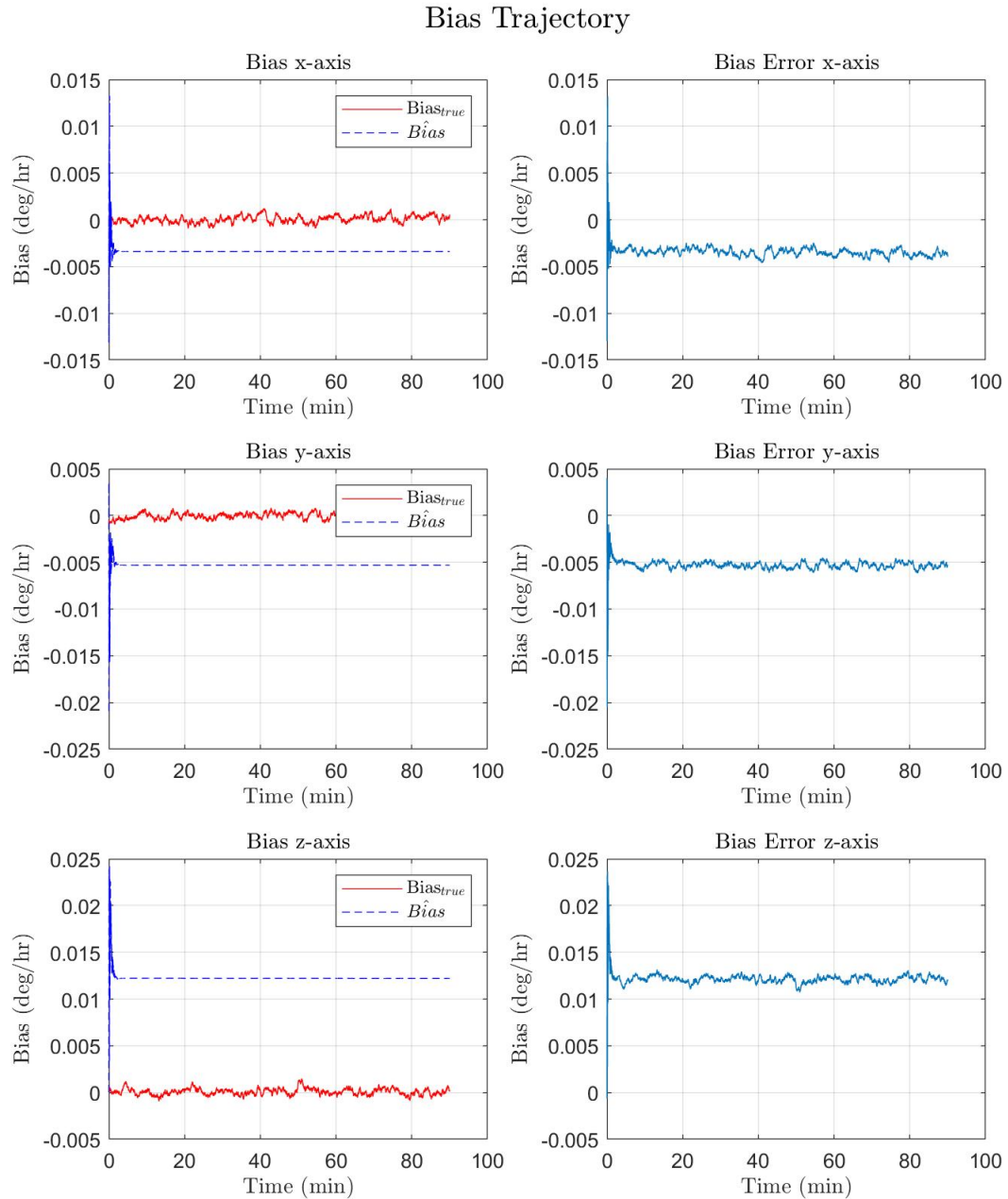


Figure 6: Deviation of the star tracker measurements

5 Conclusion

In this project, we have demonstrated that a spatial navigation system using a Multiplicative Extended Kalman Filter and equipped with a gyroscope and two star trackers can estimate the attitude of a spacecraft with an accuracy of a 0.3 arc seconds. However, the presented system was unable to accurately estimate the gyroscope biases. One valuable lesson we have learned from this work is that these systems are complex and their performance is driven by a large number of variables such as the selected sensors and their accuracy, the type of filter used, the initial conditions, the system's environment, etc. The effect of any of these variables on the performance of the proposed navigation system could be investigated in a future project.

Bibliography

- [Dev98] Christopher W. Dever. "Vehicle Model-Based Filtering for Spacecraft Attitude Determination". MA thesis. Massachusetts Institute of Technology, 1998.
- [MC14] F. Landis Markley and John L. Crassidis. *Fundamentals of Spacecraft Attitude Determination and Control*. New York: Springer, 2014. ISBN: 9781493908011.
- [Cur21] Howard D. Curtis. *Orbital Mechanics for Engineering Students*. Fourth Edition. Elsevier (Butterworth-Heinemann), 2021. ISBN: 9780128240250.
- [Le 22] Jérôme Le Ny. *ELE6209A Lecture Notes*. École Polytechnique de Montréal. 2022.
- [Wik22] Wikipedia contributors. *Sodern*. [Online; accessed 15-Apr-2022]. 2022. URL: <https://en.wikipedia.org/wiki/Sodern>.
- [XGM22] Yongchun Xie, Jianxin Guo, and Bin Meng. *Spacecraft Dynamics and Control*. Beijing Institute of Technology Press, 2022. ISBN: 9789813364479.
- [Win] Stefan Winkler. *Introduction to Spacecraft Attitude Determination*. University of Stuttgart. Satellite Control Class Notes.